

End-to-End Audio-Visual Learning for Cochlear Implant Sound Coding in Noisy Environments

Meng-Ping Lin, Enoch Hsin-Ho Huang, Shao-Yi Chien, and Yu Tsao

Abstract—The cochlear implant (CI) is a remarkable biomedical device that successfully enables individuals with severe-to-profound hearing loss to perceive sound by converting speech into electrical stimulation signals. Despite advancements in the performance of recent CI systems, speech comprehension in noisy or reverberant conditions remains a challenge. Recent and ongoing developments in deep learning reveal promising opportunities for enhancing CI sound coding capabilities, not only through replicating traditional signal processing methods with neural networks, but also through integrating visual cues as auxiliary data for multimodal speech processing. Therefore, this paper introduces a novel noise-suppressing CI system, AVSE-ECS, which utilizes an audio-visual speech enhancement (AVSE) model as a pre-processing module for the deep-learning-based ElectroNet-CS (ECS) sound coding strategy. Specifically, a joint training approach is applied to model AVSE-ECS, an end-to-end CI system. Experimental results indicate that the proposed method outperforms the previous ECS strategy in noisy conditions, with improved objective speech intelligibility scores. The methods and findings in this study demonstrate the feasibility and potential of using deep learning to integrate the AVSE module into an end-to-end CI system.

Index Terms—cochlear implant (CI), audio-visual speech enhancement (AVSE), joint training, end-to-end model

I. INTRODUCTION

The cochlear implant (CI) is a hearing device designed to help individuals with severe-to-profound hearing loss regain partial hearing. The CI system involves an external, upgradable sound processor that uses radio frequency to wirelessly link to a surgically implanted internal device. The CI system transforms speech signals into electrical pulse patterns, which are transmitted via the auditory nervous system to the auditory cortex of the brain, enabling sound perception. Developed through multidisciplinary collaboration, modern CIs now provide impressive speech recognition performance. With well-designed sound coding strategies that translate acoustic signals into electrode stimulation patterns, such as the widely used advanced combination encoder (ACE) strategy [1], most CI users can understand more than 80–90% of speech sentences

in quiet conditions [2]. However, further improvements are still needed, particularly in the processing of noisy speech.

Speech enhancement (SE) offers a potential solution for improving CI in noisy environments. With the rapid development of deep learning, SE approaches for CIs are gradually shifting from conventional signal processing algorithms to data-driven neural networks [3]–[5]. Many SE approaches have been applied to CIs, including recent end-to-end architectures [6], [7] that integrate both the pre-processing stage and the sound coding strategy [8], [9], the core component responsible for converting audio into electrical stimuli. However, these approaches, which rely solely on audio input, do not make use of the visual cues available for processing background noise and overlapping speech. In general audio applications, audio-visual speech enhancement (AVSE), a common multimodal signal processing approach, has been proposed to incorporate visual information such as lip movements and facial expressions alongside audio signals, and has proven effective in outperforming audio-only speech enhancement methods [10]–[16]. These findings encourage further exploration of visual cues and AVSE models for CI sound processing in noisy environments [17], [18].

Improving conventional CI systems with an AVSE module requires careful design to overcome associated challenges. The core signal processing functions of the ACE coding strategy, envelope detection and channel selection (CS), are not differentiable, making them difficult to integrate with neural-network-based AVSE modules and refine through data-driven regression. To overcome this limitation, the ElectroNet-CS (ECS) model introduced in [19] is used to explore the capabilities of deep-learning-based CI coding strategies. This model replicates the envelope detection and channel selection processes of the ACE strategy using a deep neural network (DNN) along with a dedicated CS function, while achieving comparable performance to ACE. The ECS coding strategy enables the integration of different front-end and post-processing components, allowing for joint training and end-to-end optimization across various tasks. Consequently, the end-to-end AVSE-ECS CI system, which involves the pre-processing AVSE module and the ECS strategy, is proposed and validated using objective evaluations.

The structure of this paper is as follows. Section II introduces the proposed AVSE-based CI system. Section III describes the experimental setup for objective evaluation. Section IV presents the results. Section V provides the conclusions.

Manuscript version August 19, 2025. (*Corresponding author: Yu Tsao.*)

M.-P. Lin is with Graduate Institute of Electronics Engineering, National Taiwan University, Taipei 106319, Taiwan.

E. H.-H. Huang is with the Research Center for Information Technology Innovation, Academia Sinica, Taipei 115201, Taiwan.

S.-Y. Chien is with Department of Electrical Engineering and Graduate Institute of Electronics Engineering, National Taiwan University, Taipei 106319, Taiwan.

Yu Tsao is with the Research Center for Information Technology Innovation, Academia Sinica, Taipei 115201, Taiwan, and also with the Department of Electrical Engineering, Chung Yuan Christian University, Taoyuan 320314, Taiwan (e-mail: yu.tsao@citi.sinica.edu.tw).

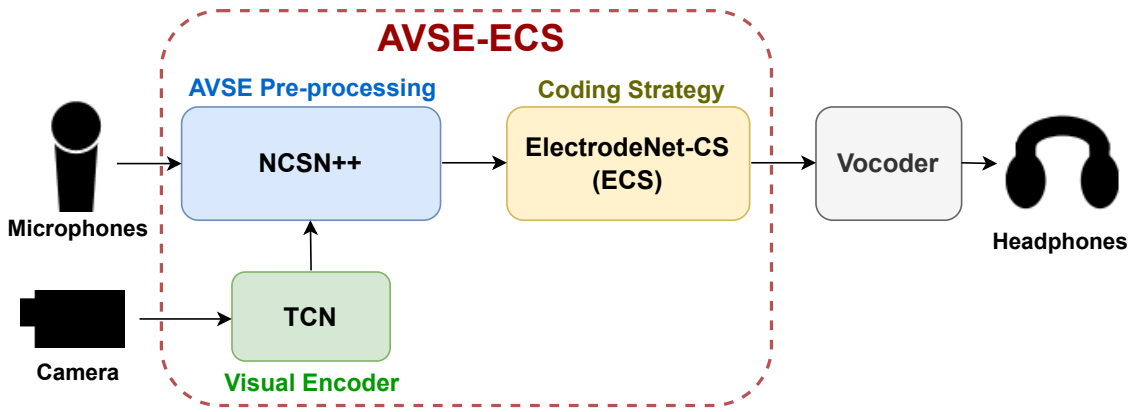


Fig. 1. The architecture of the proposed cochlear implant (CI) system. The area enclosed by the dotted line indicates the AVSE-ECS network.

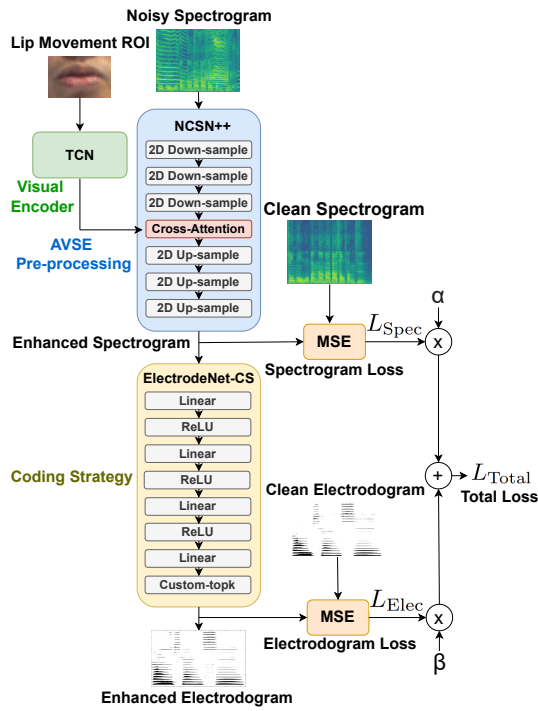


Fig. 2. Overall architecture of the training AVSE-ECS.

II. METHOD

A. System Architecture

The system architecture of the proposed AVSE-ECS CI system is illustrated in Fig. 1. The AVSE model incorporates auxiliary visual cues to generate enhanced speech, which is further processed by the ECS strategy into electrode stimulation patterns. A tone vocoder [20] is used to convert electrode stimulation patterns into audible speech, which can then be analyzed using objective evaluation methods. Furthermore, this study introduces a joint training approach, and the architecture for training the AVSE-ECS network is illustrated in Fig. 2.

B. Coding Strategy

This study adopts the DNN-based ECS model proposed in [19] as the coding strategy, which is the core sound processing of the CI system. This model consists of four dense layers with 1024, 512, 256, and 22 neurons, followed by a custom topk layer designed for the CS function. The ECS model is pre-trained before being integrated into the AVSE-ECS system. Pre-training involved paired spectral-temporal matrices across $L = 65$ bins and $M = 22$ channels derived from clean speech processed with the ACE strategy. The training was configured to preserve key information in the $N_{topk} = 8$ channels selected by the network, while distributing lower envelope data across the remaining $M - N_{topk}$ channels, using the L1 norm across all M channels.

C. Visual Encoder

The temporal convolution network (TCN) is employed as the visual encoder as illustrated in Fig. 1 and Fig. 2. This model consists of a 3D convolutional layer to process temporal sequences of frames, followed by a 2D ResNet-18. The extracted visual features are then passed to the AVSE model as visual embeddings. Note that a modified ResNet-18 visual encoder is pre-trained using the Lip Reading in the Wild (LRW) dataset [21]. To provide the most relevant visual cues for SE, the encoder focuses on the mouth, referred to as the region of interest (ROI), rather than utilizing the entire facial region. Facial landmarks are detected using the Mediapipe face tracker [22], and the mouth ROI is extracted accordingly. To reduce computational overhead during training, the visual encoder is kept frozen and the embeddings are pre-extracted, minimizing both memory usage and the number of training parameters.

D. AVSE Pre-processing

For the AVSE pre-processing, this study adopts and modifies the NCSN++ model from [23]. As this original UNet is designed for generative tasks, the timestep is set to 1 in this study, and the model's output directly serves as the enhanced speech. For audio feature preprocessing before AVSE, the

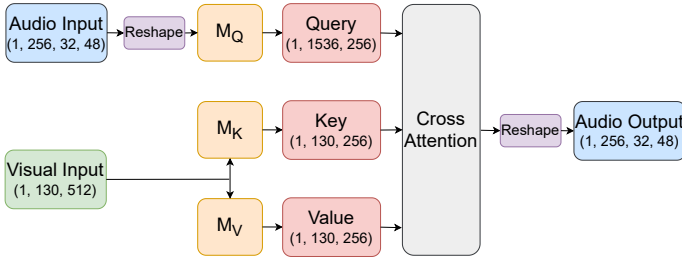


Fig. 3. The schematic diagram of the audio-visual fusion block.

experimental settings are similar to [24]. Audio signals are resampled to 16 kHz and converted into complex-valued STFT representations. Using a window size of 510 and a periodic Hann window, the resulting frequency dimension is $F = 256$. The hop length is set to 128. Each STFT spectrogram is truncated to $T = 256$ time frames, enabling random cropping during batch training.

E. Audio-Visual Fusion

This study explores the use of cross-attention blocks, illustrated by the red block in Fig. 2, to integrate audio and visual information. The attention mechanism enables neural networks to dynamically focus on the most relevant parts of the input, capture contextual dependencies, and facilitate alignment across modalities. Following a similar approach to [25], the self-attention blocks within the UNet architecture are modified by replacing the audio keys and values with visual embeddings generated by the visual encoder. Augmenting the audio input with lip movement information is intended to utilize visual cues to enhance speech reconstruction and thereby improve the overall performance of the SE system. To explain the design of the audio-visual fusion module, the cross-attention mechanism is shown in Fig. 3. Audio features (in blue) and visual features (in green) are provided as input, with dimensions indicated numerically. M_Q , M_K , and M_V represent the transformation layers for query, key, and value, respectively. They are fused by the cross attention block, then reshaped and output as audio.

F. Joint Training

Joint training in this study simultaneously optimizes both the AVSE pre-processing module, represented by the blue block in Fig. 2, and the ECS module, shown as the yellow block in Fig. 2, within an end-to-end framework. To guide the SE module toward generating high-quality enhanced speech during the learning process, a training objective called spectrogram loss is defined as follows:

$$L_{\text{Spec}} = \text{MSE}(\mathbf{E}, \mathbf{C}), \quad (1)$$

where \mathbf{E} is the enhanced speech from the AVSE model and \mathbf{C} is the clean ground truth. To consider the distance across the enhanced electrodoagram and the clean electrodoagram, the electrodoagram loss is defined as

$$L_{\text{Elec}} = \text{MSE}(\hat{\mathbf{E}}, \hat{\mathbf{C}}), \quad (2)$$

where $\hat{\mathbf{E}}$ is the enhanced electrodoagram from the AVSE-ECS model and $\hat{\mathbf{C}}$ is the clean electrodoagram from the ECS model. The clean electrodoagram is derived from the output of the ECS model when clean speech is provided as input. By narrowing the distance between the clean electrodoagram and the enhanced electrodoagram, the output electrode pattern in AVSE-ECS can be further refined, reducing the impact of input noise and improving speech intelligibility.

By considering L_{Spec} and L_{Elec} concurrently, the total loss is defined as

$$L_{\text{Total}} = \alpha * L_{\text{Spec}} + \beta * L_{\text{Elec}}, \quad (3)$$

where α and β are weights for L_{Spec} and L_{Elec} , respectively.

III. EXPERIMENTS

This section presents the experimental setups in this study.

A. Objective Evaluation Metrics

To assess the performance of CI systems, three commonly-used objective evaluation metrics are employed: short-time objective intelligibility (STOI) [26], extended short-time objective intelligibility (ESTOI) [27], and normalized covariance measure (NCM) [28], [29]. These evaluation metrics are computed based on the correlations between CI vocoded speech and clean speech to estimate speech intelligibility.

B. Dataset

The audiovisual dataset used in this study is based on the Taiwan Mandarin Hearing in Noise Test (TMHINT) speech material [30], which consists of 16 phonemically balanced lists. Each list contains 20 sentences, with each sentence consisting of 10 syllables (Chinese characters). The duration of each utterance ranges from approximately 2 to 4 seconds. The audio-only dataset and the audio-visual dataset are both based on TMHINT sentences. The audio-only TMHINT dataset is used to train the ECS model, as described in [19], with the exception that 320 clean sentences from Lists 1 to 8 are used in this study.

For training and inference of the AVSE-ECS system, the Taiwan Mandarin Speech with Video (TMSV) dataset [11], consisting of speech and video recordings of TMHINT sentences, is adopted. The method for using the TMSV dataset is similar to that described in [11]. This dataset includes speech recordings from 18 native Mandarin speakers (13 males and 5 females). In this study, considering gender balance, 8 speakers (4 male, 4 female) from TMSV are selected for training and validation. For each speaker with 320 utterances, sentences 1-190 are used for training, and sentences 191-200 for validation. These speech files are mixed with 100 types of noise [31] at 5 signal-to-noise ratio (SNR) levels (-12, -6, 0, 6, 12 dB). To reduce training time, a total of 12,000 utterances are randomly sampled. For evaluation, utterances 201-320 from two unseen speakers (1 male, 1 female) are used. These are corrupted with five noise types including music, street noise, engine noise,

baby cry, and pink noise, and mixed at SNR levels of -1, -4, -7, and -10 dB, yielding a total of 4,800 noisy utterances. The training and testing sets are fully mismatched in terms of speech content, noise types, speakers, and SNR levels to ensure robust generalization.

C. Training Configuration

According to the total loss L_{Total} introduced in Section 2.6, two types of training configurations are designed to train the AVSE-ECS Network: pre-trained and joint training. For the pre-trained method, the AVSE model is trained independently and concatenated with ECS. For the joint training method, an untrained AVSE network is connected to ECS, and the training of the full AVSE-ECS network includes the spectrogram loss L_{Spec} and the electrodogram loss L_{Elec} . The pre-trained method can be regarded as a special case of joint training, which only includes L_{Spec} in the training stage by setting $\beta = 0$. Note that in all configurations, the ECS models are pre-trained and concatenated after the AVSE model. During the joint training stage, all the parameters in ECS are frozen, and only the parameters in the AVSE model are tuned.

D. Objective Evaluation

The following three experiments are conducted for objective evaluation.

- 1) ECS with clean and noisy speech
- 2) AVSE-ECS with different β values
- 3) Comparison of ACE, ECS, ASE-ECS, AVSE-ECS

In the first experiment, an objective evaluation is conducted using the pre-trained ECS model with noisy and clean speech from the TMSV test set. This experiment examines the STOI, ESTOI, and NCM scores of the ECS model under clean and noisy conditions.

The second experiment is designed to investigate the effects of model weights during joint training on speech intelligibility. Following the pre-trained method, α is set to 1, and different values of β are explored in this experiment. The results of this experiment are used to select β for the next experiment.

The third experiment compares different CI network implementations, including ACE, ECS, ASE-ECS, and AVSE-ECS (Fig. 4). The ACE strategy is one of the most common approach based on traditional signal processing. It serves as the baseline for performance comparison. The ASE-ECS model is an audio-only system in which self-attention replaces the cross-attention mechanism used in the AVSE-ECS model. AVSE-ECS, the proposed end-to-end CI system, is evaluated using both the pre-trained method and the joint training method. For all experiments, α is set to 1, and in the joint training setup, β is set to 0.5.

IV. RESULTS

This section presents the results of the objective evaluation.

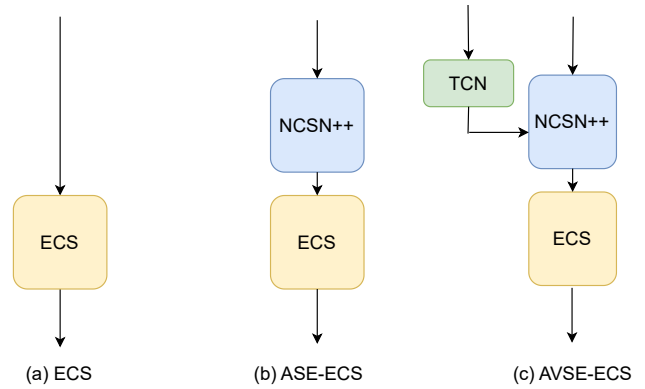


Fig. 4. The schematic comparison between different neural-network-based implementations: (a) ECS, (b) ASE-ECS), and (c) AVSE-ECS. The yellow block stands for ECS, the blue block represents the NCSN++ model, and the green block indicates the TCN visual encoder in Fig. 2.

TABLE I
OBJECTIVE EVALUATION OF THE ECS MODEL

Input Speech	STOI \uparrow	ESTOI \uparrow	NCM \uparrow
Clean	0.7604	0.5866	0.6809
Noisy	0.4870	0.2073	0.3258

A. ECS with clean and noisy speech

The objective speech intelligibility of the ECS model is evaluated with noisy and clean speech, as shown in Table I. In the absence of noise, ECS achieves an STOI score of 0.7604. Under noisy conditions, the score drops to 0.4870. Similar reductions in ESTOI and NCM scores are observed as speech transitions from clean to noisy conditions. The result shows that the performance of the ECS model declines in the noisy condition, since ECS simulates the ACE strategy without an SE approach.

TABLE II
OBJECTIVE EVALUATION OF THE AVSE-ECS NETWORK
WITH DIFFERENT β VALUES

β	STOI \uparrow	ESTOI \uparrow	NCM \uparrow
1.0	0.6196	0.3705	0.5217
0.5	0.6305	0.3899	0.5211
0.25	0.6295	0.3879	0.5199

TABLE III
OBJECTIVE EVALUATION OF DIFFERENT CI IMPLEMENTATIONS

Method	Configuration	STOI \uparrow	ESTOI \uparrow	NCM \uparrow
ACE	-	0.4870	0.2067	0.3262
ECS	-	0.4870	0.2073	0.3258
ASE-ECS	Pre-trained	0.5943	0.3557	0.4914
AVSE-ECS	Pre-trained	0.6141	0.3672	0.5067
AVSE-ECS	Joint training	0.6305	0.3899	0.5211

B. AVSE-ECS with different β values

Table II presents the objective evaluation results of AVSE-ECS with different joint training setups. Under noisy conditions, AVSE-ECS achieves an STOI score of 0.6295 ($\beta = 0.25$), 0.6305 ($\beta = 0.5$), and 0.6196 ($\beta = 1$).

Table II shows similar trends in STOI and ESTOI scores with the three β values. These results suggest that emphasizing β , the weight on the electrodogram loss, by setting it to 1 does not necessarily improve speech intelligibility. On the other hand, a smaller β value of 0.25 limits the refinement of the electrodogram. Among the tested values, $\beta = 0.5$ results in the highest STOI and ESTOI scores among the three weights. Although $\beta = 1$ achieves a slightly higher NCM score (0.5217) compared to $\beta = 0.5$ (0.5211), the difference is marginal and not considered significant. Therefore, the β value of 0.5 is selected for the subsequent experiment.

C. Comparison of ACE, ECS, ASE-ECS, and AVSE-ECS

Table III compares different CI system implementations under noisy conditions. The ECS approach achieves a STOI score of 0.4870, which is comparable to that the ACE strategy. Using the pre-trained setup, the audio-only ASE-ECS model achieves a STOI score of 0.5943, surpassing the ECS strategy without the SE module. With the addition of visual cues, the AVSE-ECS model increases the STOI score to 0.6141 in the pre-trained setting and to 0.6305 with joint training. Similar trends can be observed in the ESTOI and NCM scores.

These results demonstrate that the ECS model effectively emulates the performance of ACE, validating the feasibility of neural network-based CI systems. Furthermore, incorporating the ASE and AVSE models improves objective speech intelligibility compared to the ECS model. The use of visual cues in the AVSE-ECS model further enhances the SE capability compared to the audio-only ASE-ECS model. However, cleaner speech input does not necessarily result in CI electrode stimulation patterns with higher speech intelligibility. To address this, the proposed joint training strategy incorporates the clean electrodogram as an auxiliary training target. This additional training objective allows the AVSE model to produce enhanced speech that enables the CI system to generate electrode stimulation patterns with higher speech intelligibility. Therefore, with the joint training method, the AVSE-ECS model achieves the highest scores in this study.

D. Discussion

A few aspects can be discussed for this study. While comprehensive objective evaluations have been conducted, additional subjective listening tests are planned to assess the effectiveness of the proposed AVSE-ECS method from a human perceptual perspective. These subjective experiments are to be conducted with both normal-hearing individuals using CI simulations and actual CI users. Physiological evaluations, including responses to auditory stimuli processed by the proposed approaches, may provide objective observations in human subjects.

In this study, the objective evaluation relies on a single TMSV dataset in one language, Mandarin Chinese. As highlighted in prior studies [32]–[34], regression-based tasks such as speech enhancement and speech separation are generally less sensitive to language differences. As a result, models trained on English speech data have shown effective generalization to other languages. Moreover, to ensure the cross-language, cross-speaker, cross-dataset, and cross-validation generalizability of the proposed approach, further investigations using diverse datasets are planned. Since audiovisual datasets are less accessible than audio-only datasets, further dataset collection and development are needed in terms of size, diversity, and real-world coverage. For each dataset, multiple runs with different random seeds will be repeated to ensure the consistency and robustness of the proposed system.

Implementing AVSE processing in CI hardware poses practical challenges, especially in achieving real-time performance. The proposed AVSE system with end-to-end CI processing can be executed on a PC, making it suitable for applications with relaxed timing constraints, such as movie streaming, online courses, and playback scenarios. Real-time deployment on CI sound processors is challenging due to latency, but the system is expected to integrate with external edge devices like smartphones, tablets, or smart glasses as intermediary platforms for practical use. These devices can offload computation from the implant-side processors, enabling more advanced audiovisual processing in everyday use. Looking ahead, we plan to further reduce the model's computational footprint through techniques such as model pruning and knowledge distillation. In addition, further investigations into the NCSN++ model, the proposed AVSE backbone, will be conducted to assess the feasibility of using lightweight alternatives for hardware implementation and their seamless integration into the hearing assistance ecosystem. In the future, advances in device processing power are expected to reduce signal processing latency and make the AVSE module a feasible application.

It is worth noting to explore the end-to-end architecture. A recent study demonstrates an analogous architecture to an end-to-end neural amplifier designed for hearing aids. [35]. Future research will aim to improve the overall CI sound processing system by exploring more advanced AVSE pre-processing methods and end-to-end frameworks.

V. CONCLUSION

This paper introduces a novel end-to-end CI system, AVSE-ECS, which integrates an audio-visual speech enhancement (AVSE) model with a deep-learning-based sound coding strategy, ElectroNet-CS (ECS). This system exhibits strong noise suppression capabilities and effectively mitigates severe performance degradation of the CI in noisy environments. A joint training approach used to train the entire end-to-end system enhances electrode stimulation patterns, making them more distinct and recognizable. A series of experiments is conducted to verify the effectiveness of the proposed method. Future work includes subjective listening evaluations, cross-dataset generalization studies, and exploration of alternative

AVSE preprocessing frameworks. The methods and findings of this study may provide insights into end-to-end approaches for CI sound coding strategies based on multimodal processing, such as audio-visual integration.

REFERENCES

- [1] A. E. Vandali, L. A. Whitford, K. L. Plant, G. M. Clark, "Speech perception as a function of electrical stimulation rate: Using the Nucleus 24 cochlear implant system," *Ear Hear.*, vol. 21, no. 6, pp. 608–624, 2000.
- [2] F.-G. Zeng, S. Rebscher, W. Harrison, X. Sun, and H. Feng, "Cochlear implants: system design, integration, and evaluation," *IEEE Rev. Biomed. Eng.*, vol. 1, pp. 115–142, 2008.
- [3] Y.-H. Lai, F. Chen, S.-S. Wang, X. Lu, Y. Tsao, and C.-H. Lee, "A deep denoising autoencoder approach to improving the intelligibility of vocoded speech in cochlear implant simulation," *IEEE Trans. Biomed. Eng.*, vol. 64, no. 7, pp. 1568–1578, 2017.
- [4] F. Henry, M. Glavin, and E. Jones, "Noise reduction in cochlear implant signal processing: A review and recent developments," *IEEE Rev. Biomed. Eng.*, vol. 16, pp. 319–331, 2023.
- [5] N. Mamun and J. H. L. Hansen, "Speech enhancement for cochlear implant recipients using deep complex convolution transformer with frequency transformation," *IEEE/ACM Trans. Audio Speech Lang. Process.*, vol. 32, pp. 2616–2629, 2024.
- [6] T. Gajecski, Y. Zhang, and W. Nogueira, "A deep denoising sound coding strategy for cochlear implants," *IEEE Trans. Biomed. Eng.*, vol. 70, no. 9, pp. 2700–2709, 2023.
- [7] T. Gajecski and W. Nogueira, "Adversarial learning for end-to-end cochlear speech denoising using lightweight deep learning models," in *Proc. ICASSP 2025 – IEEE Int. Conf. Acoust. Speech Signal Process.*, pp. 1–5, Apr. 2025.
- [8] J. Wouters, H. J. McDermott, and T. Francart, "Sound coding in cochlear implants: From electric pulses to hearing," *IEEE Signal Process. Mag.*, vol. 32, no. 2, pp. 67–80, 2015.
- [9] E. H.-H. Huang, C.-M. Wu, and H.-C. Lin, "Combination and comparison of sound coding strategies using cochlear implant simulation with Mandarin speech," *IEEE Trans. Neural Syst. Rehabil. Eng.*, vol. 29, pp. 2407–2416, 2021.
- [10] S.-Y. Chuang, Y. Tsao, C.-C. Lo, and H.-M. Wang, "Lite audio-visual speech enhancement," in *Proc. Interspeech*, 2020.
- [11] S.-Y. Chuang, H.-M. Wang, and Y. Tsao, "Improved lite audio-visual speech enhancement," *IEEE/ACM Trans. Audio Speech Lang. Process.*, vol. 30, pp. 1345–1359, Feb. 2022.
- [12] J.-C. Hou, S.-S. Wang, Y.-H. Lai, Y. Tsao, H.-W. Chang, and H.-M. Wang, "Audio-visual speech enhancement using multimodal deep convolutional neural networks," *IEEE Trans. Emerg. Top. Comput. Intell.*, vol. 2, no. 2, pp. 117–128, 2018.
- [13] E. Ideli, B. Sharpe, I. V. Bajić, and R. G. Vaughan, "Visually assisted time-domain speech enhancement," in *Proc. GlobalSIP*, 2019.
- [14] A. Adeel, M. Gogate, A. Hussain, and W. M. Whitmer, "Lip-reading driven deep learning approach for speech enhancement," *IEEE Trans. Emerg. Top. Comput. Intell.*, vol. 5, no. 3, pp. 481–490, 2021.
- [15] D. Michelsanti, Z.-H. Tan, S.-X. Zhang, Y. Xu, M. Yu, D. Yu, and J. Jensen, "An overview of deep-learning-based audio-visual speech enhancement and separation," *IEEE/ACM Trans. Audio Speech Lang. Process.*, vol. 29, pp. 1368–1396, 2021.
- [16] M. Sadeghi, S. Leglaive, X. Alameda-Pineda, L. Girin, and R. Horaud, "Audio-visual speech enhancement using conditional variational auto-encoders," *IEEE/ACM Trans. Audio Speech Lang. Process.*, vol. 28, pp. 1788–1800, 2020.
- [17] R.-Y. Tseng, T.-W. Wang, S.-W. Fu, C.-Y. Lee, and Y. Tsao, "A study of joint effect on denoising techniques and visual cues to improve speech intelligibility in cochlear implant simulation," *IEEE Trans. Cogn. Develop. Syst.*, vol. 13, no. 4, pp. 984–994, 2021.
- [18] R. L. Lai, J.-C. Hou, M. Gogate, K. Dashtipour, A. Hussain, and Y. Tsao, "Audio-visual speech enhancement using self-supervised learning to improve speech intelligibility in cochlear implant simulations," *arXiv preprint arXiv:2307.07748*, 2023.
- [19] E. H.-H. Huang, R. Chao, Y. Tsao and C.-M. Wu, "ElectrodeNet—A deep-learning-based sound coding strategy for cochlear implants," *IEEE Trans. Cogn. Dev. Syst.*, vol. 16, no. 1, pp. 346–357, Feb. 2024.
- [20] M. F. Dorman, P. C. Loizou, A. J. Spahr, and E. Maloff, "A comparison of the speech understanding provided by acoustic models of fixed-channel and channel-picking signal processors for cochlear implants," *J. Speech Lang. Hear. Res.*, vol. 44, pp. 1–6, 2002.
- [21] J. S. Chung and A. Zisserman, "Lip reading in the wild," *Proc. ACCV*, 2016.
- [22] <https://github.com/google-ai-edge/mediapipe>
- [23] Y. Song, J. S.-Dickstein, D. P. Kingma, A. Kumar, S. Ermon, and B. Poole, "Score-based generative modeling through stochastic differential equations," in *Proc. ICLR*, 2021.
- [24] M.-P. Lin, J.-C. Hou, C.-W. Chen, S.-Y. Chien, J.-C. Chen, X. Lu, Y. Tsao, "Bridging the multi-modality gaps of audio, visual and linguistic for speech enhancement," *arXiv preprint, arXiv:2501.13375*, 2025.
- [25] C.-W. Chen, J.-C. Hou, Y. Tsao, J.-C. Chen, and S.-Y. Chien, "DAVSE: A diffusion-based generative approach for audio-visual speech enhancement," in *3rd COG-MHEAR Workshop on Audio-Visual Speech Enhancement (AVSEC)*, 2024.
- [26] C. H. Taal, R. C. Hendriks, R. Heusdens, and J. Jensen, "A short-time objective intelligibility measure for time-frequency weighted noisy speech," *IEEE/ACM Trans. Audio Speech Lang. Process.*, vol. 19, no. 7, pp. 2125–2136, 2011.
- [27] J. Jensen, and C. H. Taal, "An algorithm for predicting the intelligibility of speech masked by modulated noise maskers," *IEEE/ACM Trans. Audio Speech Lang. Process.*, vol. 24, no. 11, pp. 2009–2022, 2016.
- [28] I. Holube, and B. Kollmeier, "Speech intelligibility prediction in hearing-impaired listeners based on a psychoacoustically motivated perception model," *J. Acoust. Soc. Amer.*, vol. 100, no. 3, pp. 1703–1716, 1996.
- [29] R. L. Goldsworthy and J. E. Greenberg, "Analysis of speech-based speech transmission index methods with implications for nonlinear operations," *J. Acoust. Soc. Amer.*, vol. 116, no. 6, pp. 3679–3689, 2004.
- [30] L. L. Wong, S. D. Soli, S. Liu, N. Han, and M.-W. Huang, "Development of the Mandarin hearing in noise test (MHINT)," *Ear Hear.*, vol. 28, no. 2, pp. 70S–74S, 2007.
- [31] G. Hu, "100 nonspeech environmental sounds," 2004.
- [32] Y. Zhang, R. J. Weiss, H. Zen, Y. Wu, Z. Chen, R. J. Skerry-Ryan, et al., "Learning to speak fluently in a foreign language: Multilingual speech synthesis and cross-language voice cloning," *Proc. Interspeech*, pp. 2080–2084, 2019.
- [33] A. Sankar, S. Anand, P. Varadhan, S. Thomas, M. Singal, S. Kumar, et al., "IndicVoices-R: Unlocking a massive multilingual multi-speaker speech corpus for scaling Indian TTS," *Adv. Neural Inf. Process. Syst.*, vol. 37, pp. 68161–68182, 2024.
- [34] R. Chao, R. Nasretidinov, Y. C. F. Wang, A. Jukić, S.-W. Fu, and Y. Tsao, "Universal speech enhancement with regression and generative Mamba," *Proc. Interspeech*, 2025.
- [35] S. Ahmed, R. E. Zezario, H.-G. Yuan, A. Hussain, H.-M. Wang, W.-H. Chung, and Y. Tsao, "NeuroAMP: A novel end-to-end general purpose deep neural amplifier for personalized hearing aids," *arXiv preprint arXiv:2502.10822*, 2025.